549. Two-Terminal Manipulation of Masses: Application to Vibration Isolation of Passive Suspensions

Chuan Li[1,2,a], Shilong Wang[1,b], Ling Kang[1,c], Song Lei[1,d], Qibing Yu[2,e]
[1] State Key Laboratory of Mechanical Transmission, Chongqing University, Chongqing 400030, China
[2] Engineering Laboratory for Detection, Control and Integrated System,
  Chongqing Technology and Business University, Chongqing 400067, China
E-mail: [a] *chuanli@21cn.com* , [b] *slwang@cqu.edu.cn (corresponding author)* ,
[c] *lingkang@cqu.edu.cn* , [d] *lsken@163.com* , [e] *xin033212@sina.com*

Abstract. A typical mass has only one genuine terminal, through which the mass interacts a position and a force vector with the environment. This paper proposes an innovative two-terminal manipulation approach for typical masses, such as mass blocks and flywheels, so as to upgrade its topology. A prototype device of the two-terminal mass is developed for testing. The experimental result validates its free two-terminal inertial dynamic characteristics. The two-terminal mass is then applied to vibration isolation of the passive suspension. The simulation result shows that, due to the presence of the second genuine terminal, the two-terminal mass contributes the suspension better isolation performance. The presented approach provides masses more extensive applications to vibration systems.
Keywords: Passive suspension, vibration isolation, mechanical terminal, two-terminal manipulation, mass.

1. Introduction

Basic building blocks for vibration systems are mass (inertial), damping and elastic elements [1]. As is shown in Fig. 1, a damping element (e.g. spring) or an elastic element (e.g. damper) has two terminals, through which the element can interact with its environment. This interaction takes place through two vectors, a position and a force, for each terminal [2]. No matter how many nodes can be connected physically, however, a typical mass element, such as a mass block or a flywheel, has only one genuine terminal, that is, itself.
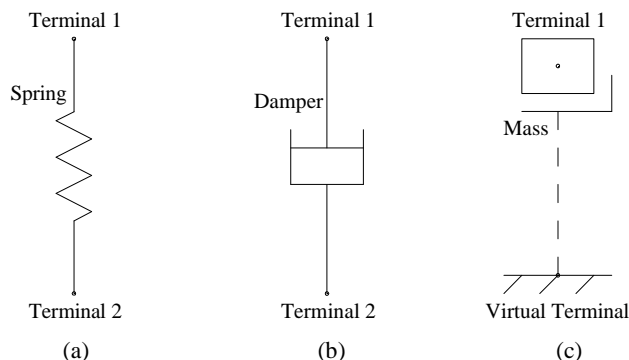
Fig. 1. Typical passive vibration elements. (a) and (b) show that there are two genuine terminals (terminal 1 and 2) available for a spring or a damper. However, as is depicted in (c), a mass has only one genuine terminal. The ground is often regarded as another virtual terminal of a mass

225

For the convenience of analysis, the ground of the inertial space is often regarded as a virtual terminal of a mass, where the position and the force are all relatively zero. In this way, unfortunately, its inertial dynamic behavior is always restricted to the ground terminal. On the one hand, the ground terminal in its topology makes that the mass can only be used for series connection in a vibration system. The parallel connection, commonly requiring two terminals, is valid only for damping and elastic elements. On the other hand, due to its topology constraint, masses are usually considered as the load entities, whereas springs and dampers, to adjust the dynamic response in vibration systems [3, 4]. But the influence of the mass on the system can not be ignored. For example, by connecting with a mass, the tuned mass damper can adjust the frequency of the vibration system with desired performance [5].

If the topology can be upgraded to be of two genuine terminals, the mass would also be wildly used for vibration control, just as springs and dampers did. Smith and et al. [6-7] designed a gear transmission flywheel, the inerter, which has two manipulation terminals for a flywheel. Rivin [8] introduced the concept of a motion transformer, which could reduce the gravitational mass while improve the inertial mass in a vibration isolation system using a screw transmission flywheel. Zhu and et al. [9] calculated a single-DOF vibration isolation system with motion transformer where 400-time virtual mass was realized. Li and et al. [10] applied a screw flywheel to the vibration control. All these researches are useful attempt to break through the terminal constraint for masses.

This research aims to improve the vibration isolation performance in terms of topology of vibration elements. To release the virtual ground terminal for the mass, an innovative two-terminal manipulation approach is introduced. The two-terminal mass is then applied to vibration isolation of the passive suspension. The presented approach would provide masses more extensive applications and better control performances in vibration systems.

2. Two-terminal manipulation approach

The topology theory is an effective tool to depict the interconnection of elements in vibration systems [11]. When the topology is employed to express a vibration system, an element is corresponding to a branch whose two nodes analogize to two terminals. Take a typical 2-DOF passive suspension model as an example. Figure 2a is the mechanical model of the system where the mass has only one genuine terminal. The disturbance is the displacement $x_0(t)$ of the tire generated by the road force $F(t)$, and the system output is the displacement $x_2(t)$ of the vehicle body m. Figure 2b shows the topology model converted from the mechanical model. In accordance with the terminal representations of springs and dampers, masses act relatively to a virtual terminal without position or force variety. Within its inertial space, the ground (node 0 in Figure 2b) is just such a terminal where the force and the position interaction with its environment are all zero.

According to the topology theory, the adjacent matrix for Fig. 2b is given by

$$\mathbf{A}_1 = \begin{matrix} & \begin{matrix} A & B & C & D & E & F \end{matrix} \\ \begin{matrix} 0 \\ 1 \\ 2 \\ 3 \end{matrix} & \begin{bmatrix} 0 & 0 & 1 & 1 & 0 & 1 \\ 0 & 0 & 0 & 0 & 1 & 1 \\ 1 & 1 & 0 & 1 & 1 & 0 \\ 1 & 1 & 1 & 0 & 0 & 0 \end{bmatrix} \end{matrix}. \tag{1}$$

Eq. (1) shows the terminal topology characteristics of masses. m_1 and m_2 have their genuine terminal 2 and 3 respectively. However, both masses have a virtual terminal at ground 0. For a typical mass such as the mass block or the flywheel, hence, the mass itself is a genuine terminal and another virtual terminal is the ground of the inertial space.

(a)   (b)
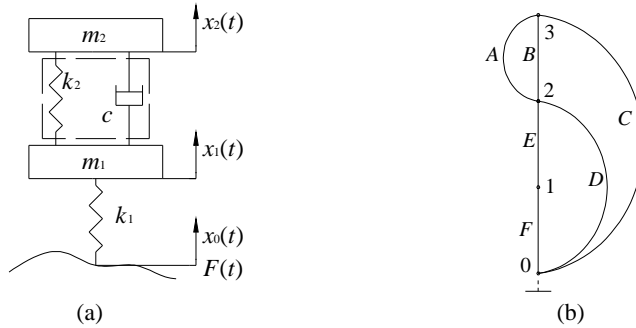
Fig. 2. A 2-DOF passive suspension system model. (a) is the mechanical model, and (b), topology model. Elements k_2, c, m_2, m_1, k_1 and $F(t)$ in (a) are respectively the corresponding objects of branches A, B, C, D, E and F in (b).

Let relative force between two terminals of a vibration element be $F=F_2-F_1$, and relative position (displacement), $x=x_2-x_1$. Because the virtual terminal is always the ground where $F_1=0$ and $x_1=0$, there is $F=F_2$ and $x=x_2$ for an arbitrary mass m, that is

$$F = F_2 = m\ddot{x} = m\ddot{x}_2. \tag{2}$$

Analyzing from the perspective of two-terminal elements [12], owing to their virtual ground terminal, masses have inertial dynamic characteristics with ground constraint. In other words, masses integrated in vibration systems have always one same terminal, that is, the ground [13]. Let's refer to Fig. 2a where m_1 and m_2 are not physically connected to the ground. But when be converted to Fig. 2b, branches C and D are all connected to node 0 and in parallel with other branches. It is obvious that masses can not be directly two-terminal connected as springs and dampers, which would restrict their applications to some extent.

In order to two-terminal connect masses with other elements in vibration systems, mechanical transmissions are considered to realize two-terminal manipulation of masses. Fig. 3 shows a rectilinear two-terminal manipulation example of the mass block.
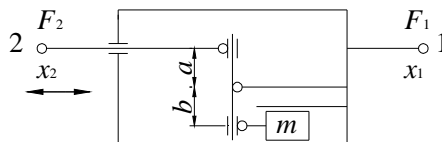
Fig. 3. Structural diagram of a simple two-terminal manipulation device

Taking no account of the structure inertia and the transmission friction, the relationship between relative force and relative displacement for foregoing device is given by

$$F = F_2 - F_1 = (b/a)m\ddot{x} = (b/a)m(\ddot{x}_2 - \ddot{x}_1). \tag{3}$$

Eq. (3) shows that the ground constraint of the mass block is released thanks to the *external structure* (lever action in Fig. 3). The inertial mass m_i of internal mass block (known as *mass core*) with its gravitational mass m is therefore

$$\begin{cases} m_i = m & b = a \\ m_i = (b/a)m & b \neq a \end{cases} \qquad (4)$$

In order to facilitate its calculation and application, we encapsulate the two-terminal manipulation of the mass to be a novel, mass-like device, namely, *two-terminal mass*. Deriving from foregoing analysis, a two-terminal mass should have following characteristics.

(1) Two free, genuine and controllable terminals. It is not necessary to fix to the ground for each terminal.

(2) Relative force $F=F_2-F_1$ between two terminals is proportional to the second-order time derivative of relative displacement (i.e. acceleration $a=a_2-a_1$) between two terminals.

(3) The inertial mass m_i of the device is proportional to the gravitational mass m of the mass core, which is related to the mechanical transmission ratio.

According to the foregoing analysis, there are also other mechanisms and mass cores available to realize two-terminal masses besides the structure shown in Fig. 3. Two basic motions, rectilinear and rotary motions, are taken into consideration for both terminals and mass cores. Tab. 1 shows 8 typical two-terminal masses with different mass cores and transmission mechanisms.

Tab. 1 Typical mass core and transmission combinations for two-terminal mass devices.

| No.	Relative motion of external terminals	Mass core	Motion transformation	Transmission mechanism
1	Rectilinear motion	Mass block	Rectilinear - Rectilinear	Lever
2	Rectilinear motion	Mass block	Rectilinear - Rectilinear	Hydraulic
3	Rectilinear motion	Flywheel	Rectilinear - rotary	Screw
4	Rectilinear motion	Flywheel	Rectilinear - rotary	Rack-gear
5	Rotary motion	Mass block	Rotary - rectilinear	Screw
6	Rotary motion	Mass block	Rotary - rectilinear	Gear-rack
7	Rotary motion	Flywheel	Rotary - rotary	Gear
8	Rotary motion	Flywheel	Rotary - rotary	Hydraulic

It is well known that the graphical symbol for a typical mass element can be depicted as Fig. 4a. Similarly, here we suggest a graphical symbol for a two-terminal mass shown in Fig. 4b, which depicts its two free terminals with mass-like dynamic characteristics.

(a)   (b)

Fig. 4 Graphical symbols of two mass devices. (a) represents the mass element and (b) is the mass-like element, the two-terminal mass

3. Experiments

According to different combinations of mass core and transmission, it is possible to develop kinds of two-terminal masses creatively. Fig. 3 which is the No. 1 combination and Fig. 5a shows the No. 3 appeared in Tab. 1. Besides combinations shown in Tab. 1, there are also other structures of two-terminal masses available for different conditions.

(a)   (b)
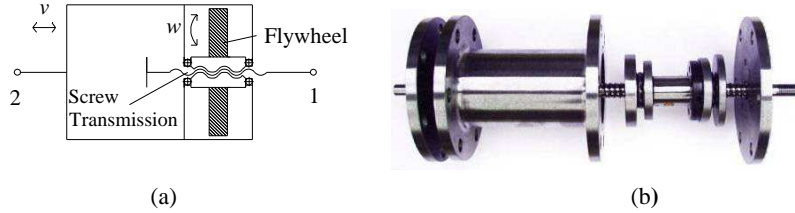
Fig. 5. A two-terminal mass with combination of the flywheel and the screw transmission. (a) shows its schematic structure. (b) is a prototype device developed in accordance with (a). The device is disassembled to show its internal mass core. Although the gravitational mass of the mass core (flywheel) is m=0.219kg, the calculated inertial mass of the device is m_i=28.5kg. Hence the device realized much bigger inertial mass m_i using much smaller actual mass core m

Fig. 5b shows a two-terminal mass prototype device designed with the flywheel and the ball screw mechanisms. Let p denote the pitch of the screw, and I denote inertia of the flywheel (mass core). F is given by [14]

$$F = I(2\pi / p)^2 \frac{dv}{dt} .$$ (5)

For a regular flywheel with gravitational mass m and radius r, rewrite above equation as

$$F = mr^2 (2\pi / p)^2 \frac{dv}{dt} .$$ (6)

Let $m_i = mr^2 (2\pi / p)^2$. It is clear that the inertial mass m_i of the two-terminal mass is $(2\pi r / p)^2$ multiples of the mass core m. For the prototype device shown in Fig. 5b, the mass core should also include the nut and the bearing besides flywheel. By theoretical calculating, the inertial mass of the device is m_i=28.5kg.

The prototype device test is performed on a PLD-20 electro-hydraulic test rig at the Engineering Laboratory for Detection, Control and Integrated System, Chongqing Technology and Business University. The device is excited by a hydraulic actuator, imposing a predefined displacement. Fig. 6 shows the test rig which holds terminals of the two-terminal mass by two hydraulic chucks. At the top of the rig, the two-terminal mass is connected to a load cell that measures the generated inertial force $F(t)$. At the bottom, the two-terminal mass is driven by the position controlled electro-hydraulic actuator of the test rig. The relative displacement of two terminals of the two-terminal mass, $x(t)$, is measured with a built-in LVDT displacement sensor. Both displacement and force signals are acquired by the data acquisition system and then transmitted to the computer for further processing. The relative acceleration $a(t)$ is not measured directly, but it can be calculated accurately based on the measured displacement when these signals are periodic.

The identification procedure for the inertial mass of the device involves the excitation of the sinusoidal signals with expected amplitudes and frequencies. Fix one terminal of the device and set desired speed of the actuator to be 123mm/s. Due to the presence of the noises in the sensing and acquisition process, the actual signals $x_0(t)$ and $F_0(t)$ should be extracted from acquired signals $x(t)$ and $F(t)$ firstly.
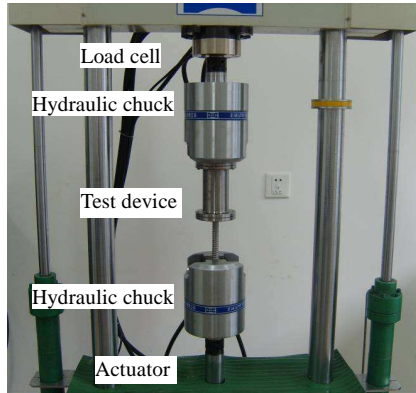
Fig. 6. The two-terminal mass mounted in the rig

There have been plenty of sophisticated signal processing algorithms recent years [15-16]. Here a simple minimum mean square error [17] fitting method is employed to identify the inertial mass m_i of the two-terminal mass.

Acquire $x(t)$ and $F(t)$, $t \in [t_0, t_0 + 2\pi]$, through the test rig of the experiment. Rewrite the actual displacement $x_0(t)$ as a standard sinusoidal signal

$$x_0(t) = n_1 \sin(n_2 t + n_3) + n_4 ,\tag{7}$$

where n_1, n_2, n_3 and n_4 are parameters to be fitted. The mean square error Δ_1 is given by

$$\Delta_1 = \frac{1}{2\pi} \sum_{t=t_0}^{t_0+2\pi} \sqrt{(x_0(t) - x(t))^2} .\tag{8}$$

Let $\min \Delta_1$ be objective function to optimize parameters in Eq. (7). With numerical optimization, $\min \Delta_1 =0.0358$mm is obtained when n_1=0.9152, n_2=0.0999, n_3=-5.5103 and n_4=14.3425. So Eq. (7) is rewritten as

$$x_0(t) = 0.9152 \sin(0.0999t - 5.5103) + 14.3425 .\tag{9}$$

Neglecting the nonlinear factors of the two-terminal mass prototype device, according to Newton's second law, the actual signal $F_0(t)$ should be

$$F_0(t) = m_i \ddot{x}_0(t).\tag{10}$$

The same minimum mean square error fitting method is used to eliminate noises from $F(t)$. Define the objective function for $F_0(t)$ as

$$\Delta_2 = \frac{1}{2\pi} \sum_{t=t_0}^{t_0+2\pi} \sqrt{(F_0(t) - F(t))^2}\tag{11}$$

Proceeding in a similar way, one can get the results $\min \Delta_2 =41.5706$N and m_i=34.1249kg when $F_0(t)$ is

$$F_0(t) = -311.6868\sin(0.0999t - 0.5505) .\tag{12}$$

230

Fig. 7a shows the comparison of $x(t)$ and $x_0(t)$. Fig. 7b shows both acquired force $F(t)$ and actual force $F_0(t)$. Comparing theoretical calculation with experimental results for the inertial mass m_i, it is worth noting that the experimental value is bigger than that of calculation. The reason is that there are nonlinear factors such as transmission error and friction of the device. However, these nonlinear factors, the influence of which is ignored, are taken as the result of the inertial mass during identification.
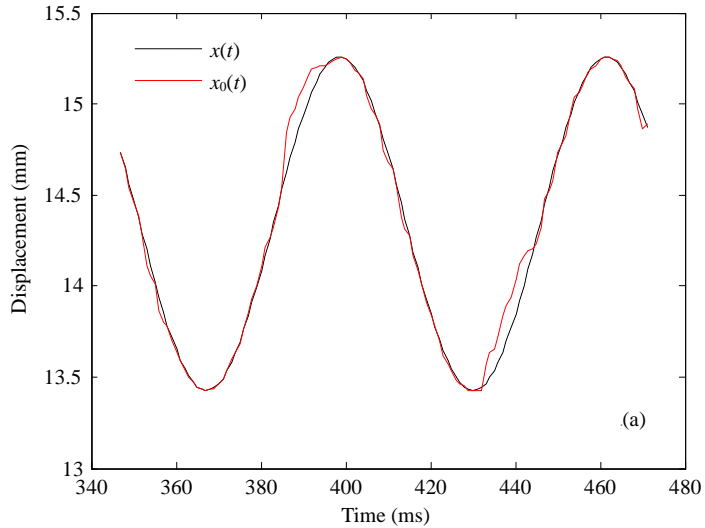
a)
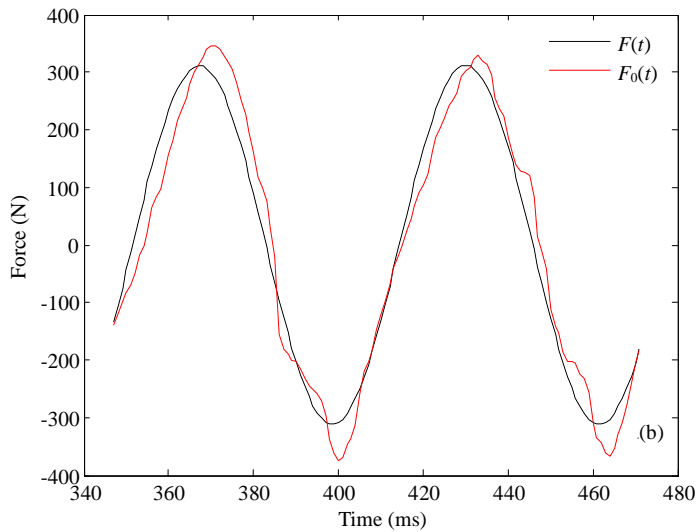
b)

Fig. 7. The displacement and the force signals of the two-terminal mass prototype device. (a) shows the displacement signals $x(t)$ and $x_0(t)$; (b) shows the force signals $F(t)$ and $F_0(t)$

Fig. 7a also indicates that there is a little error between acquired and identified displacements. However, because the two-terminal mass also magnifies nonlinear factors while magnifying the gravitational mass m of the mass core, there is a bigger fitting error for the force, which is shown in Fig. 7b.

Despite of its nonlinear factors, the experiment results validate the second-order displacement derivative dynamic characteristics of the two-terminal mass. Running like traditional rectilinear mass elements, it has two free, genuine and controllable terminals which are not included in a mass block or a flywheel.

The proposed approach offers the two-terminal mass more flexible topology property. If one of its terminals is fixed to the ground, the two-terminal mass is just a traditional mass. However, the second free terminal makes that the two-terminal mass can be integrated into vibration systems to realize more extensive applications.

4. Performance analysis in the passive suspension

Let us move back to the 2-DOF passive suspension system shown in Fig. 2. We suggest connecting a two-terminal mass m_i in parallel with k_2 and c, which is shown in Fig. 8a. The adjacent matrix of the topology shown in Fig. 8b is

$$
\mathbf{A}_2 = \begin{matrix} & \\ 0 \\ 1 \\ 2 \\ 3 \end{matrix} \begin{matrix} A & B & C & D & E & F & G \\ \begin{bmatrix} 0 & 0 & 1 & 1 & 0 & 1 & 0 \\ 0 & 0 & 0 & 0 & 1 & 1 & 0 \\ 1 & 1 & 0 & 1 & 1 & 0 & 1 \\ 1 & 1 & 1 & 0 & 0 & 0 & 1 \end{bmatrix} \end{matrix}. \tag{13}
$$
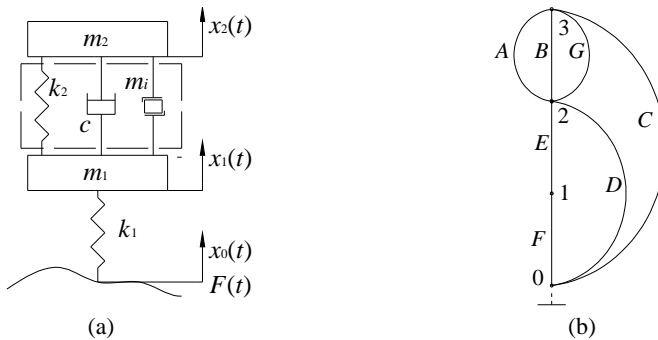
Fig. 8. A 2-DOF passive suspension model with a two-terminal mass. (a) is its mechanical model, and (b), topology. Elements k_2, c, m_2, m_1, k_1, $F(t)$ and m_i in (a) are respectively the corresponding objects of branches A, B, C, D, E, F and G in (b)

In this matrix, although columns C, D and G represent all inertial branches, their matrix elements are not all the same. Columns C and D represent traditional mass so that their elements in row 0 are 1, that is, C and D are all of one free terminal. However, column G represents the two-terminal mass without ground constraint, so that its element in row 0 is not 1. Also it can be connected in series or parallel with other vibration elements. It is worth noting that the two-terminal mass m_i, without being fixed to the ground, can not be replaced or merged by any traditional vibration components directly.

232

Desire for better performances drives the development of novel vibration isolation structures. Comparison of displacement transfers of $x_2(t)$ to m_2 of Fig. 2 and 8 would indicate the novel vibration isolation performance of the passive suspension employing the two-terminal mass.

The governing equations for the suspension model shown in Fig. 2 (S_1) are given by

$$m_2\ddot{x}_2(t) + c(\dot{x}_2(t) - \dot{x}_1(t)) + k_2(x_2(t) - x_1(t)) = 0 , \tag{14}$$

$$m_1\ddot{x}_1(t) + k_1(\dot{x}_1(t) - \dot{x}_0(t)) - c(\dot{x}_2(t) - \dot{x}_1(t)) - k_2(x_2(t) - x_1(t)) = 0 . \tag{15}$$

To discuss the performance, we consider the displacement magnification factor (DMF) of both suspensions as

$$DMF(t) = |x_2(t) / x_0(t)| . \tag{16}$$

In the Laplace domain, combining the foregoing equations, the DMF for S_1 is given by

$$DMF_1(s) = \left| \frac{k_1(k_2 + cs)}{(m_1 s^2 + k_1 + k_2 + cs)(m_2 s^2 + k_2 + cs) - (k_2 + cs)^2} \right| . \tag{17}$$

Similarly, the governing equations for isolation system shown in Fig. 8 (S_2) are

$$m_2\ddot{x}_2(t) + c(\dot{x}_2(t) - \dot{x}_1(t)) + k_2(x_2(t) - x_1(t)) + m_i(\ddot{x}_2(t) - \ddot{x}_1(t)) = 0 , \tag{18}$$

$$m_1\ddot{x}_1(t) + k_1(\dot{x}_1(t) - \dot{x}_0(t)) - c(\dot{x}_2(t) - \dot{x}_1(t)) - k_2(x_2(t) - x_1(t)) - m_i(\ddot{x}_2(t) - \ddot{x}_1(t)) = 0 . \tag{19}$$

In the Laplace domain, the DMF of S_2 is given by

$$DMF_2(s) = \left| \frac{k_1(k_2 + cs + m_i s^2)}{(m_1 s^2 + m_i s^2 + k_1 + k_2 + cs)(m_2 s^2 + m_i s^2 + k_2 + cs) - (k_2 + cs + m_i s^2)^2} \right| . \tag{20}$$

Usually the maximal DMF is one of the most important factors to be concerned for vibration isolation. Hence it is employed to define the vibration isolation performance of foregoing passive suspensions.

At first parameters of both systems should be optimized so that their performance can be compared in the same level. Fix one parameter of the model and optimize other parameter(s) so as to minimize the maximal DMF within concerned range. Let $s = j\omega$, in which $\omega \in [\omega_1, \omega_2]$ are the concerned frequency range. The performance index to measure the vibration isolation is proposed as [18]

$$J_i = \min_{m_i, c}(\max_{\omega}(DMF_i(j\omega))) , \tag{21}$$

where i represents the number of suspension models. S_1: $i=1$, S_2: $i=2$.

The following parameters are used for simulations: m_1=30kg, m_2=350kg, k_1=230×10^{3}N/m, ω_1=0Hz, ω_2=50Hz. The suspension stiffness is set as k_2=(50, 60, 70, 80, 90, 100)×10^{3}N/m. To

233

optimize the performance measures, the damping (c) and the inertial mass (m_i) are tuned to achieve the smallest values of J_i at each fixed stiffness settings (k_2). Tab. 2 shows the optimized parameters for passive suspensions S_1 and S_2 respectively. It is worth noting that m_i is the inertial mass of the two-terminal mass, which has usually much smaller gravitational mass m comparing with traditional masses.

Tab. 2 Optimized parameters for the passive suspensions S_1 and S_2 where k_2 is set as $(50\text{-}100)\times10^3$N/m

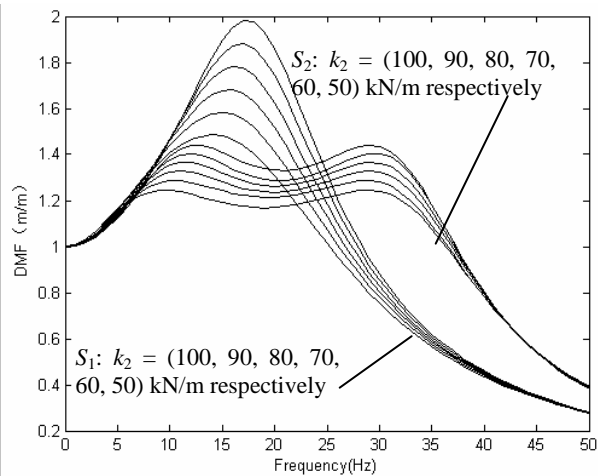| No.	Suspension S_1		Suspension S_2		
	k_2 (N/m)	C (N.s/m)	k_2 (N/m)	C (N.s/m)	m_i (kg)
1	50×10^3	7967	50×10^3	9019	214.2
2	60×10^3	8366	60×10^3	9388	229.6
3	70×10^3	8731	70×10^3	9585	249.2
4	80×10^3	9097	80×10^3	9792	267.5
5	90×10^3	9534	90×10^3	9978	286.6
6	100×10^3	9954	100×10^3	10350	300.3

With optimized parameters, J_1 and J_2 are calculated in accordance with Eq. (21). Fig. 9 shows the advantage of suggested suspension employing a two-terminal mass. With the variety of k_2 from 50 to 100 kN/m, the vibration isolation performance of S_2 improves averagely 28.89% comparing with that of S_1 in given examples.

Fig. 10 shows the DMF varieties of two suspensions within the concerned frequency range [0, 50] Hz. One can see that there is an obvious benefit in using a two-terminal mass for a passive suspension. Owing to the two-terminal manipulation of the mass, its topology is upgraded so that it can be connected in parallel with the damper and the spring. Thanks to the presence of the two-terminal mass, the resonant peaks of the suspension are all reduced remarkably at different suspension stiffness examples.

The presented two-terminal manipulation approach releases the ground terminal for the mass, which greatly expands the vibration applications in contrast with traditional masses. Besides the vibration isolation, it may also be used for other vibration applications.
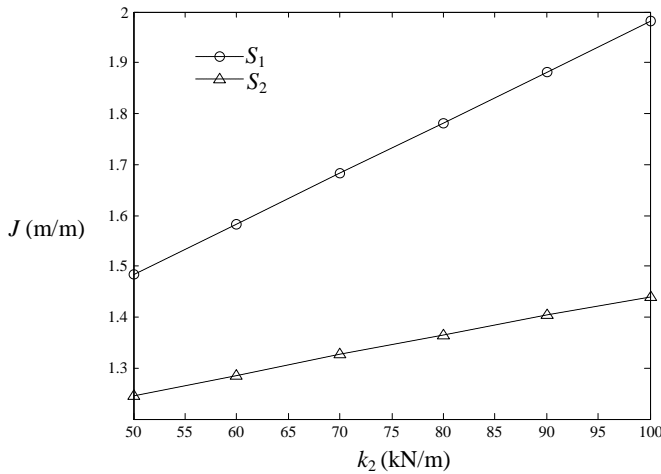
Fig. 9. Comparison of vibration isolation performances of two suspensions. The figure indicates that the vibration isolation performance (less J_i means better performance) of S_2 improves averagely 28.89% comparing with that of S_1 in given examples

234

Fig. 10. Comparison of DMF varieties of two suspensions with different values of k_2 within the concerned frequency range.

5. Conclusions

(1) A novel two-terminal manipulation approach for the mass is introduced. It may release the ground terminal of the mass and possesses the free two-terminal topology characteristics as elastic and damping elements.

(2) Different combinations of the mass core and the external structure are employed to realize two-terminal mass devices. A prototype device is developed and tested in a rig. The experiment result validates the second-order displacement derivative dynamic characteristics of the two-terminal mass.

(3) Based on the topology, the vibration isolation performances of the typical passive suspension with or without a two-terminal mass are investigated. With the optimized parameters, the simulation indicates that the suspension employing a two-terminal mass improves averagely 28.89% performance in given examples. Owing to the release of the ground terminal, the proposed approach could extend the topology characteristics of the mass, which has brighter application foreground in vibration systems.

Acknowledgements

References

[1] **H.Y. Hu.** Fundamentals of mechanical vibration. Beijing: Beihang University Press, 2005.
[2] **J. C. Willems.** Ports and terminals. Lecture Notes in Control and Information Sciences. 2010, 398: 27-36.
[3] **G. Caruso, O. B. Mekki, F. Bourquin.** Modeling and experimental validation of a new electromechanical damping device. Journal of Vibroengineering. 2009, 11(4): 617-626.
[4] **S. L. Wang, W. J. Ren, J. Zhou et al.** Study on 3D curve model of multi-stranded wire helical springs. China Mechanical Engineering. 2007, 18(11): 1269-1272.
[5] **E. Matta, A. D. Stefano.** Robust design of mass-uncertain rolling-pendulum TMDs for the seismic

235

protection of buildings. Mechanical Systems and Signal Processing. 2009, 23(1): 127-147.

[6] **M. C. Smith.** Synthesis of mechanical networks: the inerter. IEEE Transactions on Automatic Control. 2002, 47(10): 1648-1662.

[7] **C. Papageorgiou, M. C. Smith.** Positive real synthesis using matrix inequalities for mechanical networks: application to vehicle suspension. IEEE Transactions on Control Systems Technology. 2006, 14(3): 423-435.

[8] **E. I. Rivin.** Passive Vibration Isolation. New York: ASME Press, 2003.

[9] **S. J. Zhu, J. J. Lou, Q. W. He et al.** Vibration Theory and Isolation Technology. Beijing: National Defense Industry Press, 2006.

[10] **C. Li, J. L. Deng, S. L. Wang et al.** Research on the electromechanical analogy design theory of the spiral flywheel motion transformation system. Journal of Mechanical Engineering. 2010, 46(3): 103-108.

[11] **S. Y. Wang, K. Tai, S. T. Quek.** Topology optimization of piezoelectric sensors/actuators for torsional vibration control of composite plates. Smart Materials & Structures. 2006, 15(2): 253-269.

[12] **J. J. Zhang, F. Liang, Y. H. Yang, etc.** Inverse spin hall effect in two-terminal device with Rashba spin-orbit coupling. Communications in Theoretical Physics. 2009, 52(6): 1107–1112.

[13] **S. Evangelou, D. J. N. Limbeer, R. S. Sharp et al.** Control of motorcycle steering instabilities: passive mechanical compensators incorporating inerters. IEEE Control Systems Magazine. 2006, (10): 78-88.

[14] **C. Li, S. L. Wang, X. M. Zhang et al.** Analysis of vibration control performance for a novel vehicle suspension with spiral flywheel motion transformer. Journal of Vibration and Shock. 2010, in press.

[15] **I. S. Bozchalooi, M. Liang.** In-line identification of oil debris signals: an adaptive subband filtering approach. Measurement Science and Technology. 2010, 21(1): 015104.

[16] **X. Fan, M. Liang, T. Yeap.** A joint time-invariant wavelet transform and kurtosis approach to the improvement of in-line oil debris sensor capability. Smart Materials & Structures. 2009, 18(8): 085010.

[17] **M. R. Bai, P. J. Hsieh, K. N. Hur.** Optimal design of minimum mean-square error noise reduction algorithms using the simulated annealing technique. Journal of the Acoustical Society of America. 2009, 125(2): 934-943.

[18] **C. X. Li, W. L. Qu.** Optimum properties of multiple tuned mass dampers for reduction of translational and torsional response of structures subject to ground acceleration. Engineering Structures. 2006, 28(4): 472-494.

236